Stroke

CLINICAL AND POPULATION SCIENCES

Patterns of Structural Disconnection Driving Proprioceptive Deficits in Chronic Stroke

Mika Kaeja, BSc; Leila Gajiyeva, MD; Yasser Iturria-Medina, PhD; Arno Villringer, MD, PhD; Bernhard Sehm, MD, PhD; Christopher J. Steele, PhD

BACKGROUND: Stroke is a leading cause of death and disability, with proprioceptive impairments affecting up to 64% of survivors. These impairments hinder sensorimotor recovery, significantly impacting poststroke quality of life. Proprioception depends on an integrated brain network but remains underexplored due to limitations in clinical assessments, hindering links between stroke-related damage and functional deficits. We combined quantitative proprioceptive measurements (arm position matching task) with connectome-based lesion-symptom mapping to identify white matter (WM) disconnection patterns underlying proprioceptive deficits in chronic sensorimotor stroke while controlling for motor impairment.

METHODS: In this single-center observational study (Leipzig, Germany, 2015–2018), we investigated relationships between WM disconnection and proprioceptive deficits in chronic stroke survivors with paretic arm function using connectome-based lesion-symptom mapping and kinematic assessments. Lesions were manually delineated, and proprioception was quantified using the arm position matching task on the KINARM Exoskeleton. Patient-specific voxelwise WM disconnection maps were generated using the tractography-based lesion assessment standard, quantifying disconnection relative to a healthy WM connectome (n=1001; women=556; age=22–37 years). Proprioceptive scores were regressed against disconnection maps using voxelwise linear regressions (familywise error–corrected, controlled for age and sex). A secondary analysis included motor performance (visually guided reaching task) as a covariate to isolate proprioceptive-specific effects.

RESULTS: Of 42 patients, 39 had valid arm position matching data, and 38 had valid visually guided reaching data included in the analyses (women=13; age=35–81 years). Arm position matching task scores were significantly associated with WM disconnection (d=0.58–1; P<0.005 familywise error; t=3.64–6.86) in a wide range of tracts previously implicated in proprioceptive function and beyond. Crucially, these associations persisted when controlling for motor performance using visually guided reaching task scores (d=0.44–0.93; P<0.05 familywise error; t=2.69–5.72).

CONCLUSIONS: We provide evidence that proprioceptive impairments in chronic stroke may arise from network-wide WM disconnection in key tracts mediating proprioceptive function. Our findings highlight the benefits of connectome-based lesion-symptom mapping for assessing stroke-related proprioceptive deficits and offer a framework for network-informed assessments of functional impairments that could guide targeted therapies poststroke.

GRAPHIC ABSTRACT: A graphic abstract is available for this article.

Key Words: connectome ■ neuroimaging ■ proprioception ■ robotics ■ stroke

Stroke is one of the leading causes of death and disability across the globe,[1] with survivors experiencing a wide range of impairments, including sensory, motor, and cognitive deficits, which are dependent on the size and location of lesions.[2,3] Proprioception is one crucial but underexplored function that is frequently

Correspondence to: Mika Kaeja, BSc, Neural Architecture, Behaviour and Connectivity Laboratory, Department of Psychology, Concordia University, Montreal, QC H4B 1R6, Canada, Email mika.kaeja@mail.concordia.ca; or Christopher Steele, MA, PhD, Neural Architecture, Behaviour and Connectivity Laboratory, Department of Psychology, Concordia University, Montreal, QC H4B 1R6, Canada, Email christopher.steele@concordia.ca
Supplemental Material is available at https://www.ahajournals.org/doi/suppl/10.1161/STROKEAHA.125.052266.
Preprint posted on BioRxiv May 27, 2025. doi: https://doi.org/10.1101/2025.05.22.655663.
For Sources of Funding and Disclosures, see page 743.

Stroke is available at www.ahajournals.org/journal/str

Nonstandard Abbreviations and Acronyms

APM	arm position matching
FOD	fiber orientation distribution function
MRI	magnetic resonance imaging
SLF	superior longitudinal fasciculus
VGR	visually guided reaching
WM	white matter

affected by stroke, significantly impacting motor recovery and the everyday life of patients. Indeed, up to 64% of stroke survivors are affected by proprioceptive deficits,[4] which is concerning as proprioception serves a key role in re-learning motor skills and improving functional outcomes.[5] However, proprioception is difficult to accurately assess with conventional clinical tests,[6,7] leaving the impact of stroke-induced white matter (WM) disconnection on proprioceptive deficits completely unexplored. Given that proprioceptive function requires the integration of information across multiple brain regions,[8] a more holistic connectome-informed understanding of chronic stroke-related deficits is crucial for tailoring interventions to facilitate recovery.

Stroke-induced proprioceptive deficits not only affect motor coordination but also impede the ability to learn or relearn the motor skills necessary to improve functional outcomes, negatively impacting a patient's recovery trajectory, personal autonomy, and quality of life.[5] Despite the importance of proprioceptive abilities in stroke motor recovery, standard clinical tools use ordinal scales with nonindependent measures that are not easily quantifiable and, therefore, hamper direct comparisons between/across patients.[6,7] Kinematic assessments have been proposed to solve these drawbacks and can be used to accurately and quantitatively assess proprioceptive deficits and the evolution of recovery.[7,9,10] The arm position matching (APM) task,[6] conducted using the KINARM robot, is a validated tool for quantifying proprioceptive deficits in patients with stroke.[10–12] Because proprioception depends on an active motor response, it can be difficult to isolate sensory deficits from motor contributions. To help disambiguate these components, validated tasks such as visually guided reaching (VGR)[7,13] can be used alongside APM to account for motor deficits. Together, these quantitative assessments provide a more precise understanding of the neural mechanisms underlying proprioceptive disruption following stroke.

Proprioception depends on the integration of peripheral sensory input, arising from muscle spindles, joint receptors, and cutaneous receptors, with higher-order central processing.[14] This peripheral-to-central integration underscores the multisystem nature of proprioception, which depends on coordination between peripheral sensors and distributed brain networks. Within the brain, proprioception relies on the integration of information across a network of regions, including the supramarginal gyrus, superior temporal gyrus, lateral thalamus, and somatosensory cortex, which are thought to support the perception of limb position.[8,15,16] These regions are connected by key WM tracts such as the superior longitudinal fasciculus (SLF), middle longitudinal fasciculus, arcuate fasciculus, and the dorsal column of the medial lemniscus.[12,17,18] Stroke-induced damage can disrupt both gray matter regions and the underlying WM network, leading to functional impairments.[16] A connectome-based approach, which examines how local stroke damage affects the WM network beyond the lesion boundaries (ie, connectome-based lesion-symptom mapping), is, therefore, a valuable approach for understanding the global effects of damage[2,19] and is particularly relevant for analyzing proprioception due to its integrative function across the brain.[17]

While proprioception involves both peripheral input and central integration, this study specifically targets the central representation of limb position sense, focusing on how brain-level WM disconnection contributes to proprioceptive impairment following stroke. We examine how lesion-induced damage across the WM network is related to quantified deficits in proprioceptive function using connectome-based lesion-symptom mapping (tractography-based lesion assessment standard)[20] and kinematic measurements[6,13] in chronic sensorimotor stroke survivors, which, crucially, also accounts for motor deficits. Our approach provides a holistic, network-informed assessment of quantified impairments through group-level analyses of brain-behavior relationships, alongside patient-level disconnection profiles that can be directly compared across individuals. This work may provide an early step toward applying disconnectome-based insights to the development of more targeted and individualized rehabilitation strategies.

METHODS

Data Availability

Behavioral and demographic data, individual disconnectomes, and statistical analysis code will be publicly released at https://github.com/neuralabc/Structural-Proprioceptive-Disconnectome-Stroke following publication. Details for these resources are provided in the Supplemental Material. Raw neuroimaging data cannot be shared due to the ethical standards of the ethics committee of the University of Leipzig.

Clinical Population

Participants

Forty-two (16 women) patients with first-time sensorimotor ischemic stroke in the chronic stage (>6 months poststroke) were recruited from the University Hospital Leipzig Day Clinic for Cognitive Neurology in Leipzig, Germany (aged 35 to 81 years; mean=61±11 years) between 2015 and 2018. Inclusion criteria were having (1) their first sensorimotor stroke

at least 6 months previously and (2) a Fugl-Meyer upper limb (FM-UL) assessment between 20 and 58 points (detailed in Tables S1 and S2). Exclusion criteria were (1) the patient was unable to follow instructions due to neurological disease, (2) a Mini-Mental State Examination score under 24 or experiencing visual impairments, and (3) a contraindication to magnetic resonance imaging (MRI). The ethics certification for this study was granted by the University of Leipzig's Medical Faculty Ethics Committee, and participants provided written informed consent according to the Declaration of Helsinki. This observational study is reported in accordance with the STROBE (Strengthening the Reporting of Observational Studies in Epidemiology) statement for cross-sectional studies.

Apparatus

Proprioceptive and motor deficits were measured using the KINARM Exoskeleton Lab (BKIN Technologies Ltd, Kingston, ON, Canada), which records the pattern of joint movements and muscular torques produced by the upper extremities. Both upper limbs were fully supported by the robot at shoulder level, while patients moved within an integrated 2-dimensional augmented reality display, allowing for presentation and interaction with visual targets in the same plane as limb motion. Task data were collected with Dexterit-E, version 3.5.3, and analyzed with versus 3.6.2.

APM Task (Proprioceptive Assessment)

Task

The APM task[6] from the KINARM Standard Task Library (BKIN Technologies Ltd) was used as an active assessment for central limb position sense to identify proprioceptive impairments. While both arms were obstructed from view, the patient was asked to relax their affected hand and allow the robot to move it to 1 of 9 randomized locations in a 3×3 square (Figure 1). Participants were instructed to mirror-match that location in space with their unaffected hand and to notify the experimenter when they judged that they had reached the mirrored position. Patients underwent a total of 54 APM trials over the course of a single session.

Metrics

The APM summary task score was used to operationalize patients' performance, where greater scores represented greater proprioceptive impairment. The task score was calculated based on the following measured parameters by the KINARM: Absolute Error (the mean absolute distance error across all trials), variability (mean value of the standard deviations of the subject's hand position for each target), contraction/expansion ratio (ratio of the range of movement of the patients arm compared with that moved by the robot), and shift (mean difference between mirrored position of subjects arm and robot-moved arm). A full description of the measurements is provided in the KINARM Standard Test Summary, version 3.9.[21]

Task Score

Each parameter was compared with a normative model comprised of 494 (262 women) healthy participants and converted into a standardized *Z* score accounting for age, sex, and handedness.[21] Based on parameter directionality, those that had unidirectional performance indicators were transformed into zeta scores, in order for indicators of the best performance to center at 0 for all parameters. Task scores are then calculated based on the performance of healthy controls, and the root-sum-square distance of Z and Zeta scores are calculated and transformed into a *Z* score via a Box-Cox transform, which is then transformed into a 1-sided zeta statistic.[21] Task score calculation results in a nominally equal weighting for all parameters.

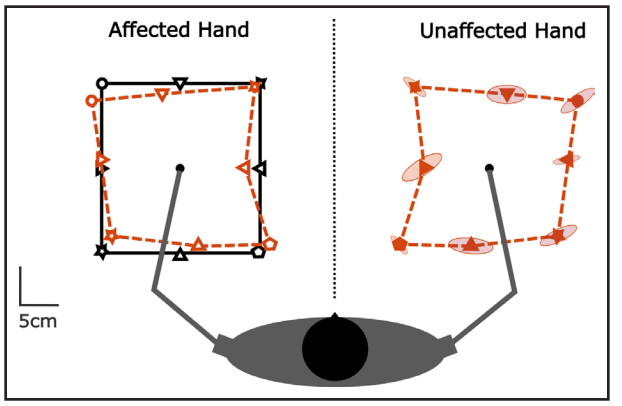

Figure 1. Arm position matching task.
This task assesses proprioception as patients use their unaffected hand (**right**) to mirror-match the position of their affected hand (**left**) after it has been moved by a robot to 1 of 9 spatial locations (black symbols). The solid orange symbols on the right represent examples of the participant's attempted matches. Accuracy in this task reflects proprioceptive function and helps assess their degree of impairment. Adapted from BKIN Technologies Ltd, 2021.

VGR Task (Motor Assessment)

Task

The VGR task[13] from the KINARM Standard Task Library (BKIN Technologies Ltd) was used as an active assessment of unilateral motor impairment. Using their arm, the patient must reach quickly and accurately from a central target to radially arranged peripheral targets, returning to the central target after maintaining their position for 3 seconds on the peripheral target.[13] Peripheral targets are distributed uniformly in a circle 90° apart, which the subject must reach 5 times in a pseudorandom order, for a total of 20 trials.[13,21]

Metrics

In the VGR task, patient performance was operationalized using the VGR task score, with greater values reflecting greater motor impairment. This score was derived from multiple kinematic parameters measured by the KINARM, including posture speed (median hand speed at rest), reaction time (time from target onset to movement initiation), initial direction angle (angular deviation between intended and actual movement direction),

Stroke. 2026;57:732–744. DOI: 10.1161/STROKEAHA.125.052266

initial distance ratio (ratio of initial movement length to total path length), speed maxima count (number of hand speed peaks), min-max speed (average difference between adjacent speed minima and maxima after peak speed), movement time, path length ratio (ratio of traveled to ideal path length), and maximum hand speed. A full description of the measurements is provided in the KINARM Standard Test Summary, version 3.9.[21]

Task Score

Each parameter was standardized against a normative data set of 291 healthy adults (166 women) who completed the Adult v2 (4-target reach out-and-back) protocol, accounting for age, sex, handedness, and robotic platform.[21] As detailed above, individual task parameters were converted to standardized Z and Zeta scores and combined into a composite Task Score using a root-sum-of-squares approach and Box-Cox transformation. This method results in nominally equal weighting across parameters, where higher scores reflect greater proprioceptive impairment. See the APM Task section for full details.

MRI Acquisition

Patients with chronic stroke from the University Hospital Leipzig Day Clinic for Cognitive Neurology were briefed about the study procedures and intent, and provided written informed consent to participate. Following the acquisition of consent, MRI scans were acquired using a 3T Siemens MRI with a 32-channel head coil (Siemens Healthineers AG, Forchheim, Germany). Acquisition sequences included T2 fluid-attenuated inversion recovery imaging (anisotropic resolution=1×0.49×0.49 mm; echo time=395), diffusion-weighted imaging (anisotropic resolution=1.72×1.72×1.7 mm), and T1-weighted imaging (isotropic resolution=1 mm; repetition time=4.21).

MRI Processing

Lesions were segmented by hand on the T2 fluid-attenuated inversion recovery imaging. Segmentations were initially performed by a doctor in training (L.G.), individually verified by a clinical neurologist (B.S.), and then binarized to form the final lesion mask for each patient. Lesions in the left hemisphere were flipped into the right for subsequent analysis. The lesion overlap between patients in Montreal Neurological Institute space, visualized using MRtrix3,[22] is shown in Figure 2. T1-weighted imaging images were linearly registered to the standardized Montreal Neurological Institute space using Advanced Normalization Tools.[23] Lesion masks were normalized to the final connectome model space by concatenating the appropriate transforms (nearest neighbor interpolation).

Connectome Model

To allow direct comparisons across individual patients, we generated a biologically plausible connectome model to serve as a quantified baseline for comparison between patients, as has previously been proposed in our[20] and others' works.[19,24]

Participants

Participants were originally recruited across the United States through the Human Connectome Project-Young Adult.[25] One thousand and one healthy young adults (556 women) aged 22 to 37 (mean=29±4) years were selected from the Human Connectome Project-Young Adult S1200 release. This age range was selected to exclude major neurodevelopmental or neurodegenerative changes. Inclusion criteria were (1) Mini-Mental State Examination score ≥29; (2) no history of psychiatric, neurodevelopmental, or neurological disorders; (3) full brain coverage in the structural MRI; and (4) imaging acquired on a 3T scanner. All participants provided written informed consent, and data were used in accordance with the WU-Minn HCP Open Access Data policy (WU-Minn HCP Consortium Open Access Data Use Terms, 2013).

MRI Acquisition

Data acquisition was performed over 2 days.[25] Scans were collected between 2012 and 2015 using a customized 3T Siemens Connectome Skyra scanner with a 32-channel head coil (Siemens Healthineers AG).[25] This scanner had a maximum gradient strength of 100 mT/m and an inner bore diameter of 56 cm.[25] Diffusion-weighted imaging (isotropic resolution=1.25 mm, repetition time=5520 ms, and echo time=89.5 ms; flip angle=78°, refocusing flip angle=160°, and field of view=210×180 mm) was acquired using a multishell protocol with 90 uniformly distributed directions and b values of 1000, 2000, and 3000 s/mm². T1-weighted imaging (isotropic

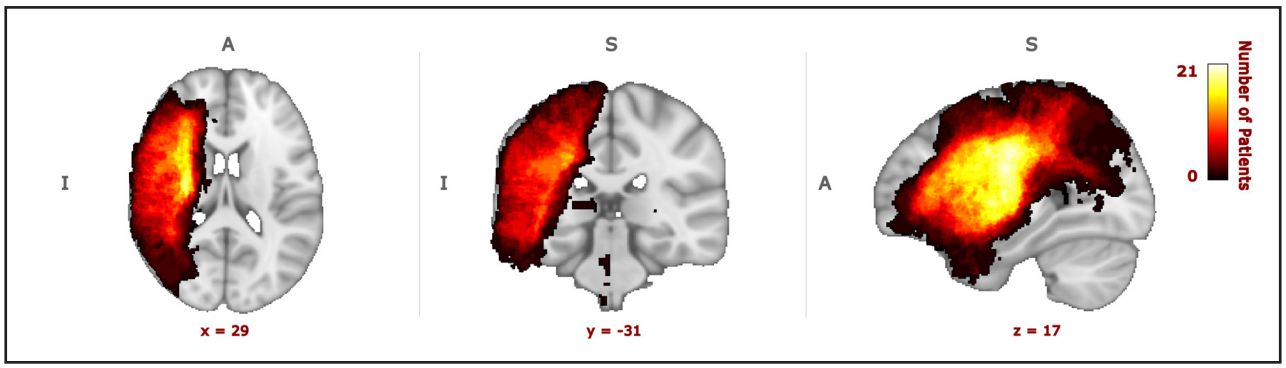

Figure 2. Lesion overlap across all patients.
Lesion overlaps across all 39 patients with arm position matching values. The area of maximal overlap is across the sensorimotor system. All lesions were flipped into the right hemisphere for analysis. The colorbar indicates lesion overlap from 1 (dark red) to 21 (bright yellow) patients. Axis labels are given as follows: A=anterior, S=superior, and I=ipsilesional hemisphere.

resolution=0.7 mm, repetition time=2400 ms, echo time=2.14 ms, flip angle=8°, and field of view=224×224 mm) was used in the construction of the connectome model.

MRI Processing

The preprocessing steps used to construct the model using MRtrix3[22] are fully described by Tremblay et al.[26] In short, T1-weighted imaging was segmented into 5 tissue types, and the minimally preprocessed diffusion-weighted imaging data were processed with constrained spherical deconvolution analysis[27] to generate fiber orientation distribution functions (FODs). FODs were used in conjunction with the 5 tissue types segmentation to perform group registration that optimized for the alignment of FODs within WM. The final connectome model was computed by performing anatomically constrained probabilistic tractography[28] on the FOD optimized group average (detailed in the Supplemental Methods). To maximize biological plausibility,[29,30] we first generated a large number of oversampled streamlines that initiated and terminated in the WM-gray matter interface (100 million). We then performed 2 sets of filtering: first selecting the 10 million most plausible streamlines[29] and then reweighting them[30] to fit the original FODs in each voxel. This process works globally to ensure that the resulting streamlines (and their associated weights) are constrained by the underlying diffusion data and are, therefore, more biologically plausible.[30]

Patient-Specific Disconnectomes

To generate patient-specific disconnectome maps, the final connectome model was first transformed from HCP space to Montreal Neurological Institute space, providing a standardized anatomic framework compatible with individual lesion masks. Each patient's lesion mask was introduced into the connectome model as an exclusion mask to remove any streamlines that would have passed through lesioned tissue. For each voxel, the number of removed streamlines was divided by the total number of streamlines passing through that voxel in the healthy connectome model, yielding the proportion of disconnection due to stroke (ie, their disconnectome).[20] As the disconnectome is computed relative to a healthy connectome model, this method can be used to compare across patients regardless of the specific lesion locations. Our approach, the tractography-based lesion assessment standard,[20] is composed of a custom-built Python script that calls specific MRtrix3 functions. Figure 3 provides a visual summary of this approach,

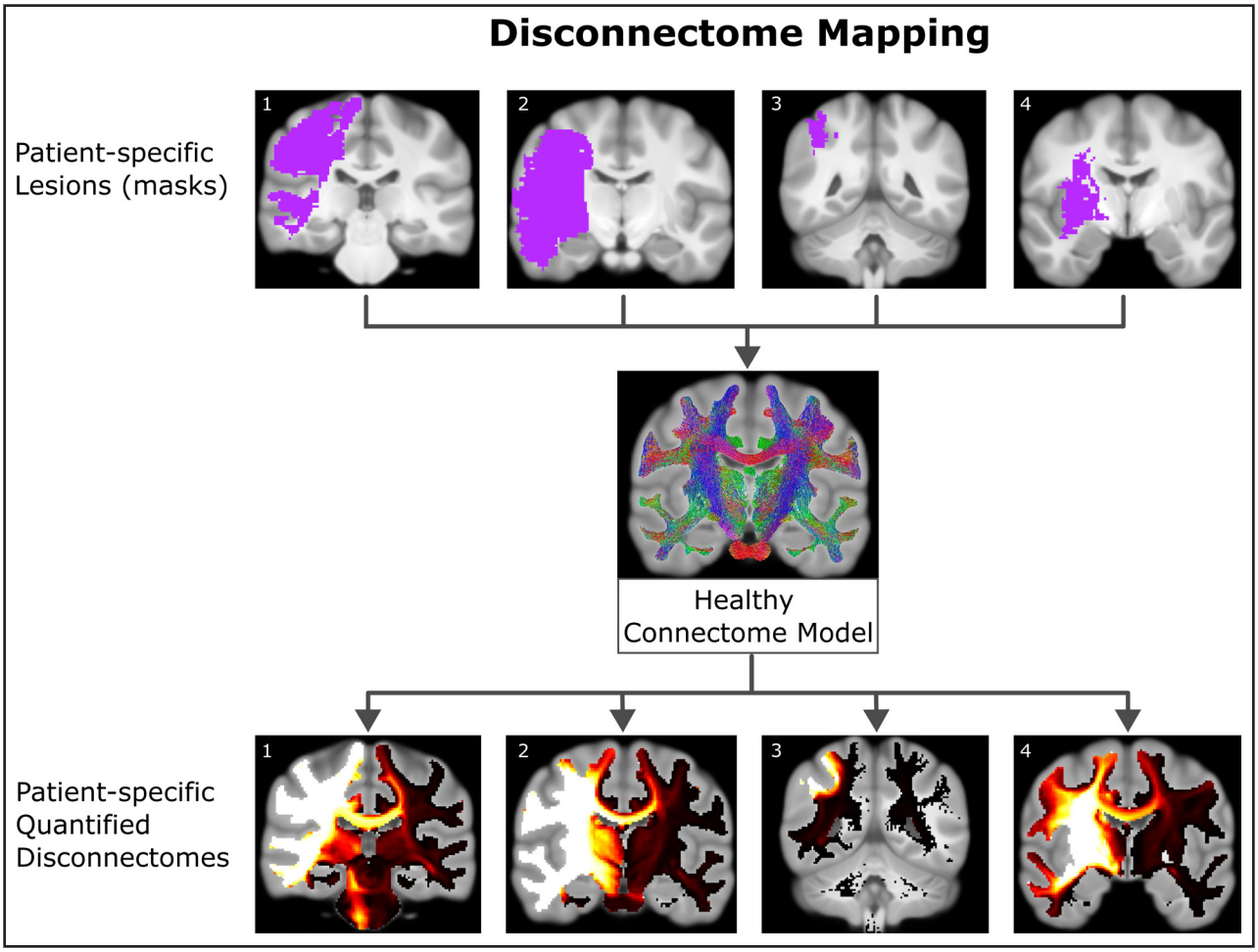

Figure 3. A visual summary of the disconnectome mapping approach with patient-specific examples.
The lesion masks of each patient (seen in purple) are individually projected into the healthy connectome model to obtain each of their quantified disconnectomes (maximum disconnection proportion in yellow-white). The corresponding numbers on the lesion masks and disconnectomes indicate the same patients. Please refer to Figure S1 for all patient disconnectomes.

 Stroke. 2026;57:732–744. DOI: 10.1161/STROKEAHA.125.052266

while further methodological details and patient-specific results are available in the Supplemental Methods and Figure S1.

Statistical Analysis

To identify WM tracts where disconnection is associated with proprioceptive deficits, we performed mass univariate voxelwise regressions in which the APM task score of the affected limb served as the dependent variable and the proportion of disconnection at each voxel as the independent variable. The task score represents a standardized summary measure of the patient's task performance relative to a healthy reference population (see Methods: APM Task [Proprioceptive Assessment]-Task Score section for complete details on score computation). Analyses were restricted to patients with complete APM task scores. These variables were entered into ordinary least-squares general linear regressions with threshold-free cluster enhancement[31] and 5000 randomized permutations using Nilearn.[32] A voxelwise familywise error correction threshold of $P<0.05$ was applied to control for multiple comparisons, with age and sex included as covariates. To further isolate disconnection patterns specific to proprioceptive impairment from those related to motor impairment, an additional analysis was conducted in which the VGR task score of the affected limb was added as an additional covariate. The VGR task score was defined in the same way as the APM task score (see Methods: VGR Task [Motor Assessment]-Task Score section), and analyses were restricted to patients with complete VGR task scores.

For both analyses, regional identification of significant clusters was made with reference to the Johns Hopkins University Diffusion International Consortium of Brain Mapping WM parcellation atlas[33] and the Thiebaut de Schotten Digital Atlas.[34] In addition, T values were converted to Cohen d values to estimate effect size, and regions with moderately strong effects (d>0.6) were subsequently presented for display using MRTrix3[22] and Nilearn.[32] Additional details for the specific functions used for the connectome-based lesion-symptom mapping analysis and tract identifications can be found in the Supplemental Methods.

Table 1. Characteristics of Patients Included in the Analysis

	n=39*
Demographics	
Age, y	58 (53–68)
Women	13 (33.3%)
Behavioral performance	
APM task score	1.6 (0.7–2.4)
VGR task score	2.8 (1.7–3.6)
Clinical characteristics	
Time since stroke, mo	47 (11–75)
NIHSS score	3 (2–4)
FM-UL score	52 (43–57)
Affected side	
Left	19 (48.7%)
Right	21 (53.8%)
Lesion features	
Lesion volume, mm³	4156 (656–24920)
Affected hemisphere	
Left	20 (51.3%)
Right	20 (51.3%)
Vascular territory	
MCA	28 (71.8%)
ICA	7 (17.9%)
PCA	6 (15.4%)
BA/VB	5 (12.8%)
AChA	9 (23.1%)
VA/PICA/ASA	1 (2.6%)

Values are n (%) or median (interquartile range) owing to nonnormal data distribution. AChA indicates anterior choroidal artery; APM, arm position matching; BA/VB, basilar/vertebrobasilar arteries; FM-UL, Fugl-Meyer upper limb; ICA, internal carotid artery; MCA, middle cerebral artery; NIHSS, National Institutes of Health Stroke Scale; PCA, posterior cerebral artery; VA/PICA/ASA, vertebral/posterior inferior cerebellar/anterior spinal arteries; and VGR, visually guided reaching.

RESULTS

The study cohort consisted of 42 patients with chronic sensorimotor stroke, of whom 39 successfully completed the APM task and 38 completed the VGR task. The demographic and clinical characteristics of the participants are described in Table 1. Lesion overlap was largest in WM underlying the sensory, motor, and premotor cortices (Figure 2). Each patient-specific disconnectome exhibited distinct disconnection patterns, which are presented for each patient in Figure S1. For completeness, we also computed the correlations between FM-UL, APM, and VGR task scores (FM-UL–APM: r=–0.66; $P=0.000005$; FM-UL–VGR: r=–0.57; $P=0.0002$; and APM–VGR: r=0.44; $P=0.006$; Table S2).

APM

Thirty-nine patients with chronic ischemic sensorimotor stroke (13 women) aged 31 to 81 (mean=59.98±11.44) years exhibited a wide range of APM performance (range: 0.01–5.39; M=1.83±1.29; refer to Table S1 for details). The analysis regressing APM task score and voxelwise disconnection values, while accounting for age and sex, revealed an extensive set of significant WM regions (d=0.58–1; $P<0.005$ familywise error; t=3.64–6.86) underlying the parietal, supplementary motor, temporal, precentral, postcentral, and supramarginal cortices (Figure 4; Figure S2; Table S3). To focus on the key WM regions supporting proprioception, we present a subset of the significant areas that exceeded a moderate effect size (d>0.61) in Table 2, which corresponds to a familywise error corrected $P<0.003$ and t>3.85.

VGR Added as a Covariate

Thirty-eight patients with chronic ischemic sensorimotor stroke (13 women; mean age=60.22±11.50 years) exhibited a wide range of VGR performance (range:

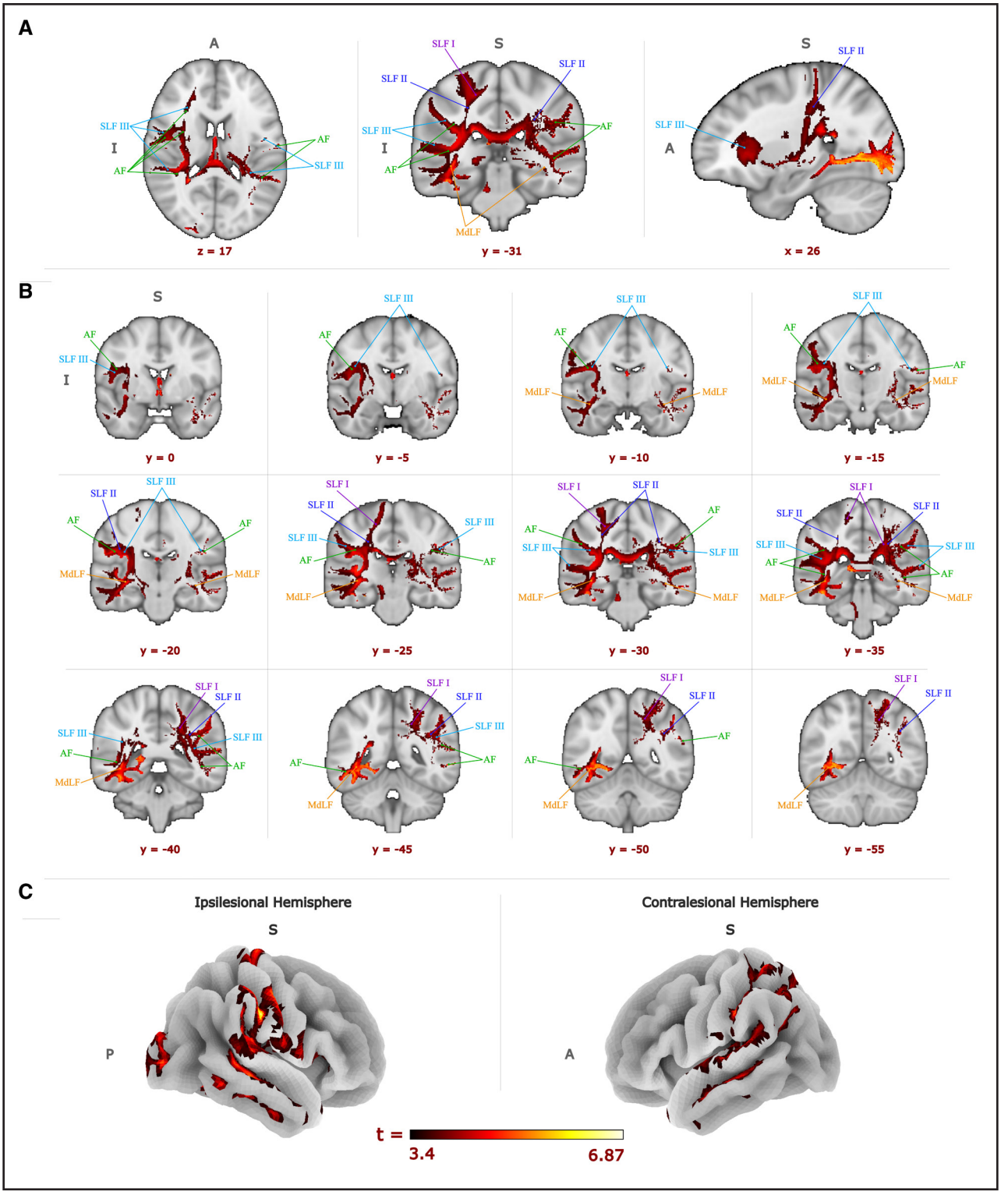

Figure 4. Voxelwise relationship between stroke-induced white matter (WM) disconnection and arm position matching (APM) performance.

Significant voxelwise t values (P<0.005; t>3.64) showing associations between APM performance and WM disconnection following sensorimotor stroke. **A**, Orthogonal views, (**B**) corresponding coronal slices, and (**C**) projected cortical surface effects, where darker colors indicate lower t values; lighter colors indicate higher t values. Each key tract is labeled and indicated on the image: superior longitudinal fasciculus (SLF) I (purple), SLF II (dark blue), SLF III (light blue), arcuate fasciculus (AF; green), and middle longitudinal fasciculus (MdLF; blue). All images are in radial convention in Montreal Neurological Institute space (mm), with the affected hemisphere on the radiological right. Axis labels are given as follows: A=anterior, P=posterior, S=superior, and I=ipsilesional hemisphere.

Table 2. Tracts Underlying the Relationship Between APM Performance and WM Disconnection While Controlled for Age and Sex

Hemisphere/ region	Classification	WM tracts
Medial	Commissural tract	Body of the corpus callosum*
		Splenium of the corpus callosum†
		Fornix (column and body)*
		Anterior commissural tract†
		Frontal commissural tract*
Bilateral hemispheres	Projection tract	Posterior limb of the internal capsule*
		Retrolenticular part of the internal capsule*
		Anterior thalamic radiation*
		Optic radiations*
	Association, commissural, and projection tract	Sagittal stratum*
	Association tract	External capsule*
		SLF I, SLF II, and SLF III*
		AF*
		MdLF*
		Anterior cingulum*
		Inferior longitudinal fasciculus*
		Inferior fronto-occipital fasciculus*
Ispilesional hemisphere	Projection tract	Anterior limb of the internal capsule†

List of WM tracts impacted by the relationship between stroke-induced WM disconnection and APM performance while controlling for age and sex post-stroke, significant at the minimum threshold of d>0.61, $P<0.003$, t>3.85 level. AF indicates arcuate fasciculus; APM, arm position matching; MdLF, middle longitudinal fasciculus; SLF, superior longitudinal fasciculus; and WM, white matter.
*$P<0.003$, †$P<0.001$.

0.94–4.86; mean=2.70±1.10; refer to Table S1 for details). The analysis regressing APM task score and voxelwise disconnection values, while accounting for age, sex, and VGR task score, revealed a set of significant WM tracts that spatially overlapped with those identified in the primary analysis (d=0.44–0.93; $P<0.05$ familywise error; t=2.69–5.72; Figure 5; Figure S3; Table S4). A subset of these tracts that exceeded a moderate effect size (d>0.47; $P<0.03$; t>2.91) is listed in Table 3.

DISCUSSION

Our proprioception-focused approach reveals, for the first time, the brain-wide structural WM disconnection patterns underlying proprioceptive deficits after sensorimotor stroke while controlling for motor impairments. By mapping patient-specific disconnection profiles, we provide evidence that proprioceptive impairments arise from disruptions across a distributed WM network, rather than localized damage to a single region. Given that proprioception requires integration across multiple brain regions,[8] our results highlight the importance of a whole-brain connectivity approach in position sense assessment. Importantly, by including VGR performance as a covariate, we were able to disambiguate proprioceptive impairment from overlapping contributions of motor impairment, further isolating the network-level substrates of central limb position sense. This framework not only deepens our understanding of stroke-related proprioceptive deficits but also may aid in identifying potential targets for intervention. Ultimately, our findings underscore the importance of precise behavioral quantification and emphasize the need to consider WM network disconnection when assessing proprioceptive impairments and designing rehabilitation strategies poststroke.

Network-Wide WM Disruptions in Poststroke Proprioception

We identified an expanded network of damaged WM tracts associated with poststroke proprioceptive impairment, reaffirming the role of previously implicated pathways while highlighting additional contributors.[12,16,17,35,36] Many of these tracts, including the SLF I, SLF II, SLF III, arcuate fasciculus, and middle longitudinal fasciculus, continued to underlie significant associations between disconnection and proprioceptive deficits even after accounting for motor impairment by adding VGR performance as a covariate. These findings align with prior work reporting associations between damage to these pathways and proprioceptive impairment. For example, Chilvers et al[12] reported that lower fractional anisotropy in the SLF II, SLF III, arcuate fasciculus, and middle longitudinal fasciculus derived from diffusion tensor imaging was associated with poorer proprioceptive performance on the APM task, a finding supported by our disconnectome analyses, which showed strong associations between damage to these pathways and proprioceptive impairments. This likely reflects disconnection within WM pathways responsible for integrating key cortical gray matter regions involved in proprioceptive awareness of limb location: the SLF links the superior parietal lobule with premotor and primary motor areas (M1); the arcuate fasciculus connects posterior temporal regions with the prefrontal cortex; and the middle longitudinal fasciculus interconnects the superior temporal gyrus and parietal regions, supporting multimodal sensory integration.[12,16,35] These salient tracts extend well beyond the boundaries of patients' lesions, suggesting that proprioceptive deficits arise from network-wide WM disconnection induced by sensorimotor stroke.

Across the global network of the brain, many tracts must function in tandem to effectively perform proprioceptive tasks.[8,12,17] Based on our findings, several projection, commissural, and association WM tracts showed significant associations between structural disconnection and proprioceptive impairment, warranting further

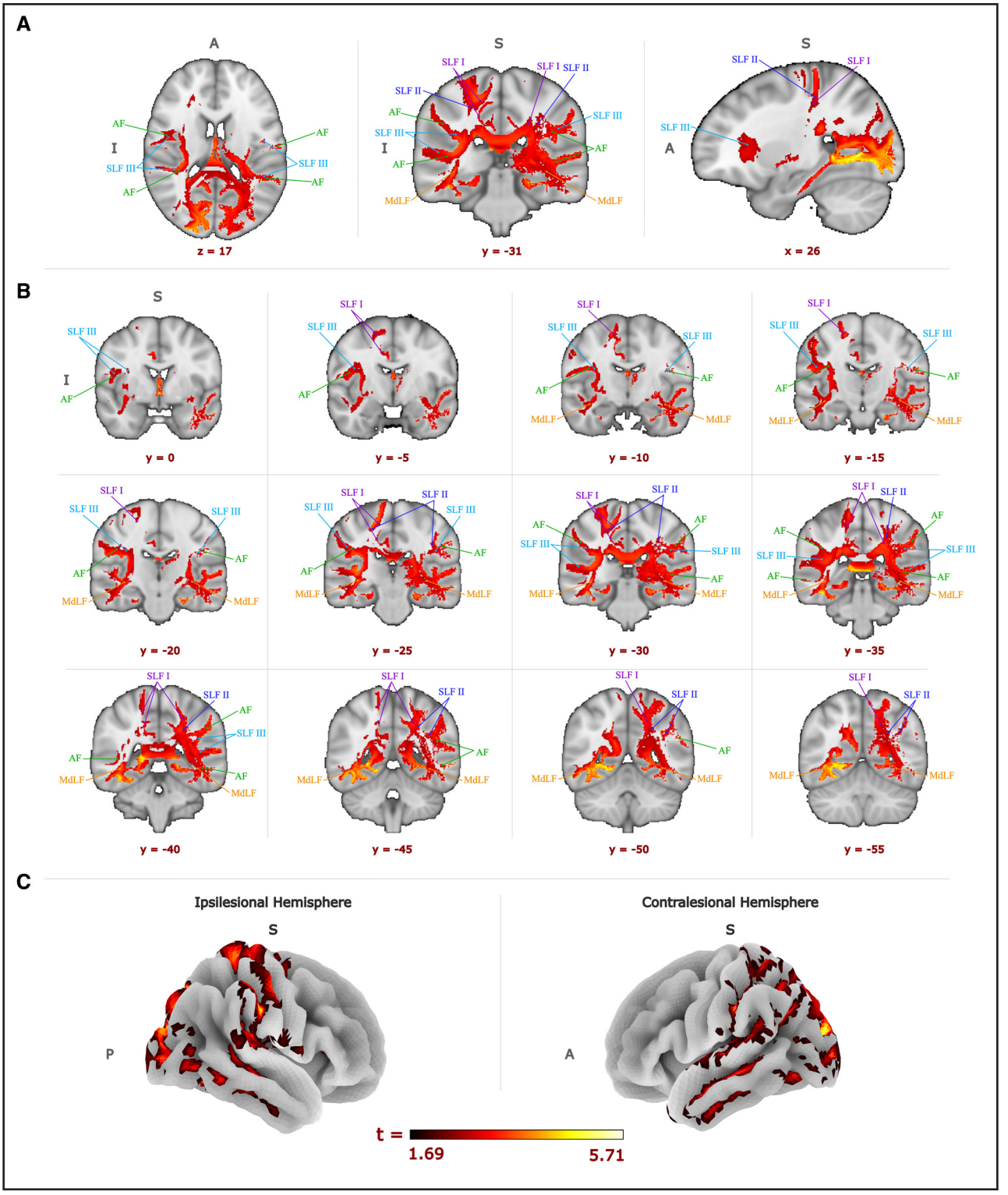

Figure 5. Voxelwise relationship between stroke-induced white matter (WM) disconnection and arm position matching (APM) performance, accounting for visually guided reaching (VGR) performance.
Significant voxelwise t values (P<0.05; t>2.69) showing associations between APM performance and WM disconnection after sensorimotor stroke, controlling for VGR performance. **A**, Orthogonal views, (**B**) corresponding coronal slices, and (**C**) projected cortical surface effects, where darker colors indicate lower t values; lighter colors indicate higher t values. Each key tract is labeled and indicated on the image: superior longitudinal fasciculus (SLF) I (purple), SLF II (dark blue), SLF III (light blue), arcuate fasciculus (AF; green), and middle longitudinal fasciculus (MdLF; blue). All images are in radial convention in Montreal Neurological Institute space (mm), with the affected hemisphere on the radiological right. Axis labels are given as follows: A=anterior, P=posterior, S=superior, and I=ipsilesional hemisphere.

Table 3. Tracts Underlying the Relationship Between APM Performance and WM Disconnection While Controlled for Age, Sex, and VGR Performance

Hemisphere/ region	Classification	WM tracts
Medial	Commissural tract	Body of the corpus callosum‡
		Splenium of the corpus callosum*
		Tapetum of the corpus callosum‡
		Fornix (column and body)†
		Anterior commissural tract†
		Frontal commissural tract‡
Bilateral hemispheres	Projection tract	Posterior limb of the internal capsule‡
		Retrolenticular part of the internal capsule‡
		Posterior thalamic radiation†
		Anterior thalamic radiation‡
		Optic radiations†
	Association, commissural, and projection tract	Sagittal stratum†
	Association tract	External capsule‡
		SLF I, SLF II, and SLF III‡
		AF‡
		MdLF†
		Anterior cingulum‡
		Posterior cingulum†
		Uncinate fasciculus‡
		Inferior longitudinal fasciculus†
		Inferior fronto-occipital fasciculus†
Contralesional hemisphere	Projection tract	Cerebral peduncle‡
		Fornix (crescent)‡

List of WM tracts impacted by the relationship between stroke-induced WM disconnection and APM performance while controlling for age, sex, and VGR performance post-stroke, significant at the minimum threshold of $d>0.47$, $P<0.03$, $t>2.91$ level. AF indicates arcuate fasciculus; APM, arm position matching; MdLF, middle longitudinal fasciculus; SLF, superior longitudinal fasciculus; VGR, visually guided reaching; and WM, white matter.

*$P<0.005$, †$P<0.01$, ‡$P<0.03$.

investigation into their roles in poststroke proprioceptive dysfunction. First, we found that damage to the medial lemniscus and spinothalamic tracts, both key ascending pathways known to transmit proprioceptive and somatosensory information, was significantly associated with proprioceptive scores in our stroke cohort. Although these tracts have been theoretically linked to proprioception,[37] our results provide the first direct evidence of their involvement in poststroke proprioceptive deficits. In addition, our proprioceptive analysis regressing APM performance on disconnection, while controlling for age and sex, revealed significant associations with a wide expanse of WM tracts. These included projection pathways such as the posterior limb, anterior limb, and retrolenticular part of the internal capsule alongside the anterior thalamic radiation and optic radiations; commissural tracts including the body and splenium of the corpus callosum, fornix (column and body), anterior, and frontal commissural tract; association pathways such as the external capsule, anterior cingulum, inferior longitudinal fasciculus, and inferior fronto-occipital fasciculus; and WM adjacent to subcortical structures such as the caudate nucleus, thalamus, pallidum, and amygdala. Almost all of these tracts, aside from the anterior limb of the internal capsule, also overlapped with significant pathways identified in our secondary analysis, accounting for motor impairment. Additional pathways revealed from the secondary analysis included the tapetum of the corpus callosum, posterior thalamic radiation, posterior cingulum, uncinate fasciculus, cerebral peduncle, crescent of the fornix, and hippocampus. These tracts, many of which are known to support sensorimotor integration, interhemispheric communication, and related cognitive and limbic processes, likely contribute to the integrity of the poststroke proprioceptive network.[38–41] Notably, while the ipsilesional hemisphere showed more focal associations with classical ascending sensory pathways, we also identified contralesional network-level disconnections consistent with diaschisis, involving widespread commissural, association, and projection pathways. The presence of these effects suggests that contralesional contributions may play a meaningful role in proprioceptive outcomes, and their structurally disconnected pathways warrant further investigation as components of the extended network underlying poststroke proprioceptive deficits. Together, our results suggest that poststroke proprioceptive function may rely on a distributed network of commissural, association, and projection pathways, several of which have not been previously highlighted in this context.

Toward Patient-Centered Rehabilitation

To fully understand the impact of lesions on proprioception, it is essential to integrate insights from both individual patient-specific disconnectomes and group-level analyses. Patient-specific disconnectomes reveal the precise WM pathway(s) disrupted in each patient, highlighting unique damage profiles that may underlie complex behavioral deficits. In parallel, the group-level analyses delineate the core tracts that link poststroke WM disconnection to proprioceptive impairment across the group, providing an anatomic framework for interpreting these deficits. Because lesions vary greatly in size and location, incorporating patient-specific disconnection patterns into clinical frameworks could support more tailored rehabilitation approaches. For instance, 2 individuals with severe proprioceptive deficits and comparable Fugl-Meyer scores may differ in which components of the impaired proprioceptive network are

affected, suggesting that their optimal rehabilitation strategies could also differ. Insights from the group-level network can help prioritize key tracts to target through therapy, while patient-specific disconnectomes can identify spared proprioceptive pathways that may compensate for lost connections. Given the critical role of rehabilitation in poststroke recovery and long-term quality of life, disconnectome-informed intervention planning may provide a valuable avenue for improving functional outcomes.[42]

Limitations, Implications, and Future Directions

A limitation of our approach is that disconnections were inferred indirectly using a connectome-based normative model rather than measured with subject-specific diffusion imaging. Disconnectomes were computed relative to a normative structural connectome derived from high-resolution diffusion MRI data in healthy young adults. While these data are of high quality, they may reflect biases related to the diffusion MRI data, the tractography method, and the normal young adult brain. However, because all patient disconnectomes were computed relative to the same normative model, comparisons across patients are internally consistent and subject to shared sources of bias and error.[43] Importantly, this connectome-based approach also offers clinical applicability, as it enables disconnection estimation from a lesion mask alone, without requiring diffusion imaging. Lesion masks can be derived from routinely acquired clinical scans, including computed tomography, 1.5T, or 3T structural MRI, making this method feasible in a wide range of clinical and research settings.

Beyond these methodological limitations, the generalizability of our findings may also be constrained by sample selection bias and imaging context. This study included chronic ischemic stroke survivors with persistent sensorimotor impairments with a limited range of FM-UL scores. Consequently, our findings may be specific to patients within this functional range and may not extend to those with substantially milder or more severe deficits. It remains to be determined whether the relationships between disconnection and behavior identified here are consistent in patients with hemorrhagic stroke or in the acute and subacute phases of recovery. This distinction is particularly important because the present results reflect the chronic stage of recovery when significant neural reorganization may have already occurred.

Quantifying individual patient-specific disconnections that result from specific lesion locations can serve as a useful guide toward developing targeted rehabilitative approaches. Knowledge of each patient's disconnectome, considered within the context of their deficits, can be used to develop a comprehensive neurorehabilitation regimen using physical (bimanual training),[44] mental (cognitive training), medical (activity modulating drugs), and technologically assistive (brain-computer interface, deep brain stimulation, noninvasive brain stimulation, and robotic training)[45–47] techniques that target WM tracts (and their linked cortical regions) most affected in each patient. Such a regimen could engage residual or alternative pathways, including those in the contralesional hemisphere, which remain structurally intact but functionally underutilized. While the tractography-based lesion assessment standard does not measure plasticity or reorganization directly, strengthening connectivity along these preserved routes may support functional improvements in some individuals. We can additionally look longitudinally at the association between the effectiveness of rehabilitation techniques and individual patterns of disconnection with their resulting impairments. This approach could be used to create a predictive model of the most effective rehabilitation techniques to create a personalized rehabilitation program based on their pattern of disconnection and associated behavioral deficits. In this way, commonly available imaging measurements (ie, lesion masks) could give practitioners insight into predicted stroke outcomes and the most effective interventions early in recovery.[48]

Conclusions

This study is the first to disambiguate proprioceptive impairment from the involvement of motor deficits using disconnectome-based analyses, allowing for a more specific investigation of the structural substrates of central limb position sense. We examined how stroke-induced WM disconnection relates to proprioceptive deficits in individuals with chronic sensorimotor stroke, using individualized disconnectome maps to perform a group-level analysis across heterogeneous lesion profiles. This revealed a network-level pattern of disconnection associated with impaired proprioceptive function. Our findings align with existing literature about the relationships between proprioceptive deficits and WM disconnection,[12,16,17,35,36] and significantly extend this work by isolating the proprioceptive-specific deficit network from motor influences, emphasizing the role of WM connections between relevant gray matter regions, and identifying additional candidate pathways for future investigation. Our results provide strong evidence that behavioral deficits are differentially affected by the location of lesions and their resulting WM disconnections. While we do not infer individual-level proprioceptive networks, this approach allows for the comparison of patient-specific disconnection patterns and the identification of common structural pathways associated with impairment. Ultimately, this research supports the use of disconnectome mapping to identify group-level network substrates of behavioral deficits among patients with differing lesion locations.

 Stroke. 2026;57:732–744. DOI: 10.1161/STROKEAHA.125.052266

ARTICLE INFORMATION

Received May 20, 2025; final revision received November 4, 2025; accepted November 10, 2025.

Affiliations

Neural Architecture, Behaviour and Connectivity Laboratory, Department of Psychology, Center for Studies in Behavioral Neurobiology and School of Health, Concordia University, Montreal, QC, Canada (M.K., C.J.S.). Department of Neurology, Max Planck Institute for Human Cognitive and Brain Sciences, Leipzig, Germany (L.G., A.V., B.S., C.J.S.). Department of Neurology and Neurosurgery, McGill University, Montreal, QC, Canada (Y.I.-M.).

Acknowledgments

The authors would like to thank the patients at the Max Planck Institute for Human Cognitive Brain Science Neurology Clinic for allowing the use of their data for this study. The authors also thank Zaki Alasmar for assistance with the pilot methodology of this project.

Sources of Funding

This research was funded by operational grants received by Dr Steele from the Natural Sciences and Engineering Research Council of Canada (DGECR-2020-00146), the Canadian Institutes of Health Research (HNC 170723), the Canada Foundation for Innovation John R. Evans Leaders Fund (project number 43722), the Heart and Stroke Foundation of Canada (National New Investigator), and the Fonds de Recherche du Québec – Santé (https://doi.org/10.69777/349443).

Disclosures

None.

Supplemental Material

Supplemental Methods
Tables S1–S2
Figures S1–S3
Reference 49

REFERENCES

1. Feigin VL, Brainin M, Norrving B, Martins S, Sacco RL, Hacke W, Fisher M, Pandian J, Lindsay P. World Stroke Organization (WSO): global stroke fact sheet 2022. *Int J Stroke*. 2022;17:18–29. doi: 10.1177/17474930211065917
2. Gleichgerrcht E, Fridriksson J, Rorden C, Bonilha L. Connectome-based lesion-symptom mapping (CLSM): a novel approach to map neurological function. *Neuroimage Clin*. 2017;16:461–467. doi: 10.1016/j.nicl.2017.08.018
3. Wist S, Clivaz J, Sattelmayer M. Muscle strengthening for hemiparesis after stroke: a meta-analysis. *Ann Phys Rehabil Med*. 2016;59:114–124. doi: 10.1016/j.rehab.2016.02.001
4. Connell L, Lincoln N, Radford K. Somatosensory impairment after stroke: frequency of different deficits and their recovery. *Clin Rehabil*. 2008;22:758–767. doi: 10.1177/0269215508090674
5. Kiper P, Baba A, Agostini M, Turolla A. Proprioceptive based training for stroke recovery. Proposal of new treatment modality for rehabilitation of upper limb in neurological diseases. *Arch Physiother*. 2015;5:6. doi: 10.1186/s40945-015-0007-8
6. Dukelow SP, Herter TM, Moore KD, Demers MJ, Glasgow JI, Bagg SD, Norman KE, Scott SH. Quantitative assessment of limb position sense following stroke. *Neurorehabil Neural Repair*. 2009;24:178–187. doi: 10.1177/1545968309345267
7. Scott SH, Lowrey CR, Brown IE, Dukelow SP. Assessment of neurological impairment and recovery using statistical models of neurologically healthy behavior. *Neurorehabil Neural Repair*. 2023;37:394–408. doi: 10.1177/15459683221115413
8. Goble DJ, Coxon JP, Van Impe A, Geurts M, Doumas M, Wenderoth N, Swinnen SP. Brain activity during ankle proprioceptive stimulation predicts balance performance in young and older adults. *J Neurosci*. 2011;31:16344–16352. doi: 10.1523/JNEUROSCI.4159-11.2011
9. Semrau JA, Herter TM, Scott SH, Dukelow SP. Robotic identification of kinesthetic deficits after stroke. *Stroke*. 2013;44:3414–3421. doi: 10.1161/STROKEAHA.113.002058
10. Semrau JA, Herter TM, Scott SH, Dukelow SP. Inter-rater reliability of kinesthetic measurements with the KINARM robotic exoskeleton. *J Neuroeng Rehabil*. 2017;14:42. doi: 10.1186/s12984-017-0260-z
11. Chilvers MJ, Hawe RL, Scott SH, Dukelow SP. Investigating the neuroanatomy underlying proprioception using a stroke model. *J Neurol Sci*. 2021;430:120029. doi: 10.1016/j.jns.2021.120029
12. Chilvers MJ, Low TA, Dukelow SP. Beyond the dorsal column medial lemniscus in proprioception and stroke: a white matter investigation. *Brain Sci*. 2022;12:1651. doi: 10.3390/brainsci12121651
13. Coderre AM, Zeid AA, Dukelow SP, Demmer MJ, Moore KD, Demers MJ, Bretzke H, Herter TM, Glasgow JI, Norman KE, et al. Assessment of upper-limb sensorimotor function of subacute stroke patients using visually guided reaching. *Neurorehabil Neural Repair*. 2010;24:528–541. doi: 10.1177/1545968309356091
14. Han J, Waddington G, Adams R, Anson J, Liu Y. Assessing proprioception: a critical review of methods. *J Sport Health Sci*. 2016;5:80–90. doi: 10.1016/j.jshs.2014.10.004
15. Bernard-Espina J, Beraneck M, Maier MA, Tagliabue M. Multisensory integration in stroke patients: a theoretical approach to reinterpret upper-limb proprioceptive deficits and visual compensation. *Front Neurosci*. 2021;15:646698. doi: 10.3389/fnins.2021.646698
16. Kenzie JM, Findlater SE, Pittman DJ, Goodyear BG, Dukelow SP. Errors in proprioceptive matching post-stroke are associated with impaired recruitment of parietal, supplementary motor, and temporal cortices. *Brain Imaging Behav*. 2019;13:1635–1649. doi: 10.1007/s11682-019-00149-w
17. Chilvers MJ, Low T, Rajashekar D, Dukelow SP. White matter disconnection impacts proprioception post-stroke. *PLoS One*. 2024;19:e0310312. doi: 10.1371/journal.pone.0310312
18. Kalambogias J, Yoshida Y. Converging integration between ascending proprioceptive inputs and the corticospinal tract motor circuit underlying skilled movement control. *Curr Opin Physiol*. 2021;19:187–193. doi: 10.1016/j.cophys.2020.10.007
19. Bonilha L, Nesland T, Rorden C, Fillmore P, Ratnayake RP, Fridriksson J. Mapping remote subcortical ramifications of injury after ischemic strokes. *Behav Neurol*. 2014;2014:215380. doi: 10.1155/2014/215380
20. Zayed A, Iturria-Medina Y, Villringer A, Sehm B, Steele CJ. Rapid quantification of white matter disconnection in the human brain. *Annu Int Conf IEEE Eng Med Biol Soc*. 2020;2020:1701–1704. doi: 10.1109/EMBC44109.2020.9176229
21. BKIN Technologies Ltd. KINARM Standard Tests Summary. 2021. Accessed October 24, 2022. https://kinarm.com/download/kst-summary-analysis-version-3-9/
22. Tournier J-D, Smith R, Raffelt D, Tabbara R, Dhollander T, Pietsch M, Christiaens D, Jeurissen B, Yeh C-H, Connelly A. MRtrix3: a fast, flexible and open software framework for medical image processing and visualisation. *Neuroimage*. 2019;202:116137. doi: 10.1016/j.neuroimage.2019.116137
23. Avants BB, Tustison NJ, Song G. Advanced normalization tools (ANTS). *Insight J*. 2009;2:1–35. doi: 10.54294/uvnhin
24. Foulon C, Cerliani L, Kinkingnéhun S, Levy R, Rosso C, Urbanski M, Volle E, Thiebaut de Schotten M. Advanced lesion symptom mapping analyses and implementation as BCBtoolkit. *GigaScience*. 2018;7:1–17. doi: 10.1093/gigascience/giy004
25. Van Essen DC, Smith SM, Barch DM, Behrens TEJ, Yacoub E, Ugurbil K; WU-Minn HCP Consortium. The WU-Minn human connectome project: an overview. *Neuroimage*. 2013;80:62–79. doi: 10.1016/j.neuroimage.2013.05.041
26. Tremblay S, Alasmar Z, Pirhadi A, Carbonell F, Iturria Y, Gauthier C, Steele C. MVComp toolbox: MultiVariate Comparisons of brain MRI features accounting for common information across metrics. *Aperture Neuro*. 2024;4:001c118427. doi: 10.52294/001c.118427
27. Jeurissen B, Tournier J-D, Dhollander T, Connelly A, Sijbers J. Multi-tissue constrained spherical deconvolution for improved analysis of multi-shell diffusion MRI data. *Neuroimage*. 2014;103:411–426. doi: 10.1016/j.neuroimage.2014.07.061
28. Smith RE, Tournier J-D, Calamante F, Connelly A. Anatomically-constrained tractography: improved diffusion MRI streamlines tractography through effective use of anatomical information. *Neuroimage*. 2012;62:1924–1938. doi: 10.1016/j.neuroimage.2012.06.005
29. Smith RE, Tournier J-D, Calamante F, Connelly A. SIFT: spherical-deconvolution informed filtering of tractograms. *Neuroimage*. 2013;67:298–312. doi: 10.1016/j.neuroimage.2012.11.049
30. Smith RE, Tournier J-D, Calamante F, Connelly A. SIFT2: enabling dense quantitative assessment of brain white matter connectivity using streamlines tractography. *Neuroimage*. 2015;119:338–351. doi: 10.1016/j.neuroimage.2015.06.092
31. Smith SM, Nichols TE. Threshold-free cluster enhancement: addressing problems of smoothing, threshold dependence and

localisation in cluster inference. *Neuroimage*. 2009;44:83–98. doi: 10.1016/j.neuroimage.2008.03.061
32. Abraham A, Pedregosa F, Eickenberg M, Gervais P, Mueller A, Kossaifi J, Gramfort A, Thirion B, Varoquaux G. Machine learning for neuroimaging with scikit-learn. *Front Neuroinform*. 2014;8:14. doi: 10.3389/fninf.2014.00014
33. Hua K, Zhang J, Wakana S, Jiang H, Li X, Reich DS, Calabresi PA, Pekar JJ, van Zijl PCM, Mori S. Tract probability maps in stereotaxic spaces: analyses of white matter anatomy and tract-specific quantification. *Neuroimage*. 2008;39:336–347. doi: 10.1016/j.neuroimage.2007.07.053
34. Rojkova K, Volle E, Urbanski M, Humbert F, Dell'Acqua F, Thiebaut de Schotten M. Atlasing the frontal lobe connections and their variability due to age and education: a spherical deconvolution tractography study. *Brain Struct Funct*. 2016;221:1751–1766. doi: 10.1007/s00429-015-1001-3
35. Findlater SE, Desai JA, Semrau JA, Kenzie JM, Rorden C, Herter TM, Scott SH, Dukelow SP. Central perception of position sense involves a distributed neural network – evidence from lesion-behavior analyses. *Cortex*. 2016;79:42–56. doi: 10.1016/j.cortex.2016.03.008
36. Findlater SE, Hawe RL, Mazerolle EL, Al Sultan AS, Cassidy JM, Scott SH, Pike GB, Dukelow SP. Comparing CST lesion metrics as biomarkers for recovery of motor and proprioceptive impairments after stroke. *Neurorehabil Neural Repair*. 2019;33:848–861. doi: 10.1177/1545968319868714
37. Biga LM, Bronson S, Dawson S, Harwell A, Hopkins R, Kaufmann J, LeMaster M, Matern P, Morrison-Graham K, Oja K, et al. 14.5 Sensory and Motor Pathways. In: *Anatomy & Physiology*. OpenStax, Oregon State University; 2019. Accessed February 24, 2025. https://open.oregonstate.education/aandp/chapter/14-5-sensory-and-motor-pathways/
38. Baumgartner P, El Amki M, Bracko O, Luft AR, Wegener S. Sensorimotor stroke alters hippocampo-thalamic network activity. *Sci Rep*. 2018;8:15770. doi: 10.1038/s41598-018-34002-9
39. Emos MC, Khan Suheb MZ, Agarwal S. Neuroanatomy, internal capsule. In: *StatPearls*. Treasure Island (FL): StatPearls Publishing; 2023. Accessed March 10, 2023. http://www.ncbi.nlm.nih.gov/books/NBK542181/
40. Goldstein A, Covington BP, Mahabadi N, Mesfin FB. Neuroanatomy, corpus callosum. In: *StatPearls*. Treasure Island (FL): StatPearls Publishing; 2023. Accessed April 27, 2023. http://www.ncbi.nlm.nih.gov/books/NBK448209/
41. Kumral E, Calli C. External and extreme capsular stroke: clinical, topographical and etiological patterns. *Cerebrovasc Dis*. 2006;21:217–222. doi: 10.1159/000091217
42. Wang Y, Liu G, Hong D, Chen F, Ji X, Cao G. White matter injury in ischemic stroke. *Prog Neurobiol*. 2016;141:45–60. doi: 10.1016/j.pneurobio.2016.04.005
43. Talozzi L, Forkel SJ, Pacella V, Nozais V, Allart E, Piscicelli C, Pérennou D, Tranel D, Boes A, Corbetta M, et al. Latent disconnectome prediction of long-term cognitive-behavioural symptoms in stroke. *Brain*. 2023;146:1963–1978. doi: 10.1093/brain/awad013
44. Yeganeh Doost M, Orban de Xivry J-J, Bihin B, Vandermeeren Y. Two processes in early bimanual motor skill learning. *Front Hum Neurosci*. 2017;11:618. doi: 10.3389/fnhum.2017.00618
45. Krakauer JW. Motor learning: its relevance to stroke recovery and neurorehabilitation. *Curr Opin Neurol*. 2006;19:84–90. doi: 10.1097/01.wco.0000200544.29915.cc
46. Laffont I, Bakhti K, Coroian F, van Dokkum L, Mottet D, Schweighofer N, Froger J. Innovative technologies applied to sensorimotor rehabilitation after stroke. *Ann Phys Rehabil Med*. 2014;57:543–551. doi: 10.1016/j.rehab.2014.08.007
47. Lefebvre S, Dricot L, Laloux P, Desfontaines P, Evrard F, Peeters A, Jamart J, Vandermeeren Y. Increased functional connectivity one week after motor learning and tDCS in stroke patients. *Neuroscience*. 2017;340:424–435. doi: 10.1016/j.neuroscience.2016.10.066
48. Lin DJ, Cloutier AM, Erler KS, Cassidy JM, Snider SB, Ranford J, Parlman K, Giatsidis F, Burke JF, Schwamm LH, et al. Corticospinal tract injury estimated from acute stroke imaging predicts upper extremity motor recovery after stroke. *Stroke*. 2019;50:3569–3577. doi: 10.1161/STROKEAHA.119.025898
49. Raffelt DA, Tournier J-D, Smith RE, Vaughan DN, Jackson G, Ridgway GR, Connelly A. Investigating white matter fibre density and morphology using fixel-based analysis. *Neuroimage*. 2017;144:58–73. doi: 10.1016/j.neuroimage.2016.09.029